Journal of Applied Chemistry JAC http://chemistry.journals.semnan.ac.ir

Investigation of photo-catalytic effect of SnO_2/AC nanocomposite on photo-degradation of basic yellow 13 and rodamin b dyes

Bahareh Fahimirad, Alireza Asghari*, Maryam Rajabi

Department of Chemistry, Semnan University, Semnan 35195-363, Iran

Article history:
Received:03/Mar/2017
Received in revised form: 17/Jun/2017
Accepted: 29/Jun/2017

Abstract

In this study, the degradation of the two dyes basic in their binary mixture is examined under the light irradiation in the presence of catalyst. A mercury lamp, which was located at a distance 30 cm from the solution surface, was used as the UV irradiation source. The first-order derivative spectra was used to obtain the residual concentration of each dye in mixtures after a given time of photo-degradation. The and techniques are employed to confirm the nanocomposite prepared. The effects of the parameters involved in the photo-catalytic activity including the solution, catalyst dosage, and concentrations of the two dyes are studied. The results obtained show that under the optimum experimental conditions and after 60 minutes of the UV light irradiation in the presence of the 8 mg catalyst and in the of 5.5, the percentage degradation of the two dyes are more than 90%.

Keywords: Photo-degradation, SnO_2/Ac nanoparticles, Derivative spectrophotometric method.

1. Introduction

Heterogeneous photo-catalysis is an emerging technique for environmental remediation, where a semi-conductor is used as the photo-catalyst [1]. The semi-conductor photo-catalyst generates electron and hole pairs upon irradiation by light above a threshold, which is a characteristic of the semi-conductor [2].

Tin oxide (SnO_2) is one of the most attractive photo-catalysts due to its high physico-chemical stability, low cost, and lack of toxicity [3-5]. It is an n-type transparent semi-conductor with a rutile structure. SnO_2 is photo-catalytically active only under the UV light irradiation with a wide band gap energy of 3.6 eV. In addition, the rapid recombination of the photo-induced electron–hole pairs hinders the practical application of SnO_2 in the photo-catalysis [6].

*.**Corresponding Author:** Associate professor of analytical chemistry. *E-mail address: aasghari@semnan.ac.ir*

Dyes and pigments represent one of the problematic groups. They are disposed into wastewaters from various industrial branches, mainly from the dye manufacturing and textile finishing as well as food-coloring, cosmetics, paper, and carpet industries [7, 8]. The photo-degradation process has been used in the recent years as a promising method for the removal of dye contaminants from industrial wastewaters since it not only degrades the pollutants but also causes their complete mineralization to CO_2, H_2O, and mineral acids [9-11].

Table 1. Basic dyes examined

Chemical structure	Commercial name
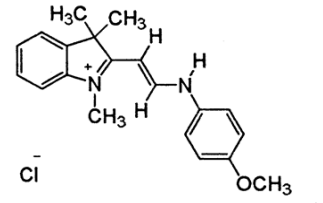	Basic yellow 13
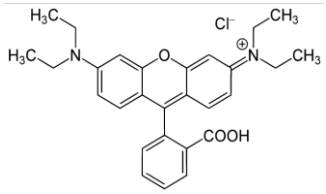	Rodamine b

In the photo-degradation of the dyes, due to highly overlapping spectra, the normal spectrophotometric method cannot perform a quantitative analysis of the binary and ternary dye solutions. The derivative spectrophotometry technique is a good and well-known procedure to resolve this limitation. The derivative spectrophotometry can simultaneously analyze multi-component dye mixtures without initial separation or purification [12, 13]. In this study, the SnO_2/AC nanocomposite was successfully prepared, which was then characterized using the powder X-ray diffraction (XRD) and scanning electron microscopy (SEM) techniques. The photo-catalytic activity of the SnO_2/AC nanocomposite was applied for first time for photodegradation of the binary mixture of the basic yellow 13 (BY13) and rodamin b (RB) dyes. In this research work, due to the overlapping absorption spectra of the solution of the dyes, the derivative spectrophotometry technique was used.

2. Experimental procedure

2. 1. Materials and method

BY13 and RB were purchased from Daystar Firm. The chemical structures of these dyes are shown in Table 1. HCl, NaOH, $SnCl_2.2H_2O$ and CH_3COOH with high purity were purchased from Merck. In all the experiments performed, doubly distilled water was used.

2.2. Instruments

The morphologies of the SnO_2 nanoparticles and the SnO_2/AC nanocomposite were determined by scanning electron microscopy (SEM; Hitachi S-4,160). The X-ray diffraction (XRD) patterns were recorded on an automated Philips X'Pert X-ray diffractometer with Cu Ka radiation (40 kV and 30 mA).The absorbance spectra of the BY13 and RB dyes were measured on a Shimadzu UV-visible 1650 PC spectrophotometer using a pair quartz cell in the range of 200-800 nm.

2.3. Preparation of SnO_2/AC

2.3.1. Synthesis of SnO_2

The SnO_2 nanoparticles were synthesized according to the literature [14]. A total of 30 mL solution of $SnCl_2.2H_2O$ (0.01 mol L^{-1}) was added to H_2O (50 mL). Then the solution pH was adjusted to 5 using CH_3COOH (1 M). 10 mL of tri ethanol amine (1 mol L^{-1}) was added to the solution, while the solution was stirred vigorously under an N_2 atmosphere. Then the solution pH was adjusted to 6using CH_3COOH (1 M). After adjusting the temperature of the solution to the room temperature, the nanoparticles were isolated and washed with ethanol, and then dried under air for 4h. Finally, the SnO_2 nanoparticles obtained were calcined in 500ºC for 1h.

2.3.2. Synthesis of SnO_2/AC nanoparticles

For synthesis of the SnO_2/AC nanoparticles during the previous step, 0.5 g of SnO_2 prepared was dispersed in H_2O (1000 mL). 10 g of activated carbon was added to it, and the resulting mixture was stirred for 12 h. Then it was filtered and washed with distilled water. Finally, the nanocomposite obtained was dried at 110 ^oC in oven for 1h [14].

2.3.3.Photo-degradation of dyes in binary solution

In this work, the photo-catalytic experiments were carried out in a photo-reactor. A 400-W mercury lamp, which was located at a distance 30 cm from the solution surface, was used as the UV irradiation source. The photo-catalytic test of the dyes in the binary solution was carried out at certain initial concentrations, with a neutral pH of the binary dye solution and a defined mass of the photo-catalyst. In order to achieve the adsorption-desorption equilibrium, the solution was stirred for 40 min at dark. Then the UV lamp was switched on, while the solution was stirred magnetically. Finally, the residual dye concentrations were measured spectrophotometrically at fixed time intervals.

The photo-degradation percentage of each dye (E%) was calculated by:

$$(E\%) = \frac{C_0 - C_t}{C_0} * 100 \qquad (1)$$

where C_0 (mgL^{-1}) is the initial concentration of the dyes after adsorption-desorption equilibrium at dark (t = 0), and C_t ($mg\ L^{-1}$) is the concentration of the dyes during the reaction time (min) [15].

2.4. Determination of concentrations of dyes by derivative spectrophotometric method

To determine the proper lambda values in the accurate analysis of the dyes in single and binary solutions, the zero-and first-order derivative spectra were used, respectively. Fig. 1 shows the zero- and first-order derivative spectra of the dyes (with the concentration of 5 $mgL^{-1}$for each dye) in single and binary solutions. As shown in this figure, the candidate lambda values for the quantitative measurement of the dyes in the binary dye system can be 374 and 569 for BY13 and RB, respectively. According to Fig. 2 The accuracy of the obtained lambda values via the first-order derivative spectrophotometric method was confirmed by corresponding the calibration curves in the concentration limits of 1-15 and 1-25 mgL^{-1} for the binary solutions of BY13 and RB in the wavelength of 374 and 569 nm, respectively. The Origin Pro 9.1 software was used to take the first-order derivative spectra of the dyes.

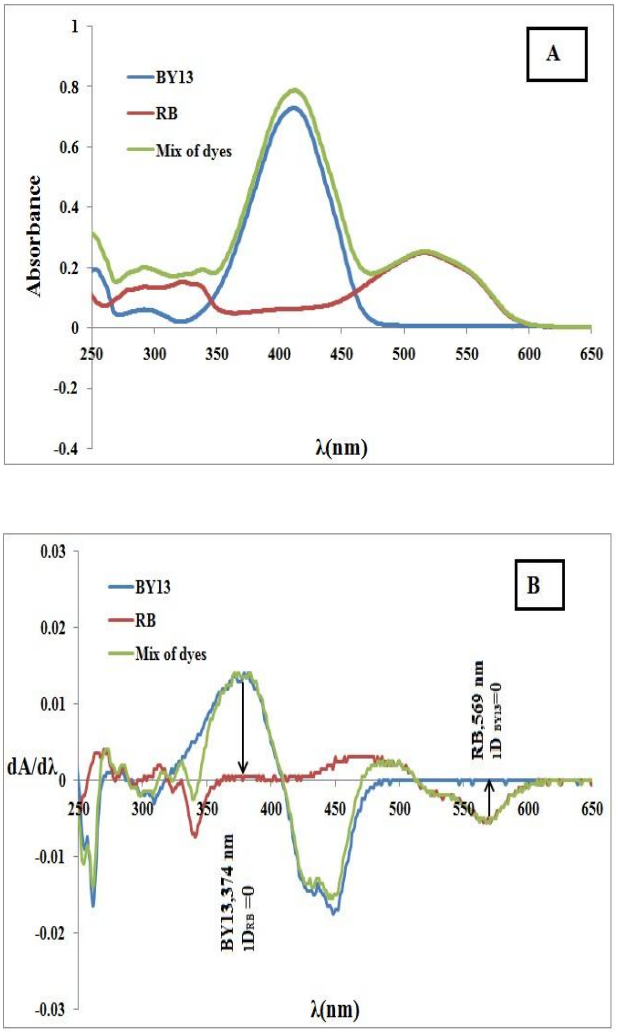

Fig.1. (A) Zero-order absorption spectra and (B) first-order absorption spectra for BY13 and RB in single and binary dye solutions, respectively.

3. Results and discussion

3.1. Characterization

Fig.3 shows the XRD patterns for the prepared nanocomposite. As shown in this figure, there is a reasonable agreement between the XRD pattern of the

prepared SnO_2/AC nanocomposite and its reference pattern. The average size of crystals was calculated using the Scherer's equation [16]:

$$d = \frac{k\lambda}{D\cos\theta} \quad (2)$$

where k, λ, θ, and D are the shape factor with the value 0.9, X-ray wavelength (0.1504 nm), Bragg's angle, and experimental full-width at half of the maximum intensity (FWHM), respectively. According to the formula, the average crystal size obtained was 60 nm [14]. The surface morphologies of the AC and SnO_2/AC nanocomposites are shown in Figs.4a and 4b. The SEM image for AC shows that the particles are well-uniformed (Fig. 4a). According to Fig.4b, SnO_2 particles are well-dispersed on the activated carbon without any aggregation. The average size of SnO_2 particles was 60 nm.

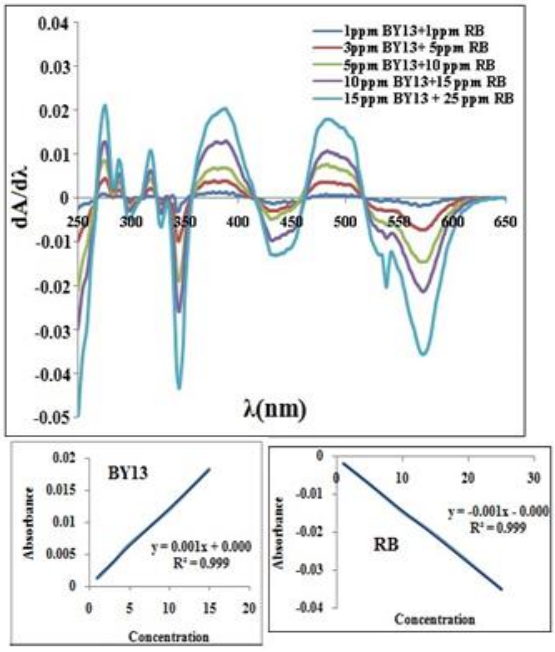

Fig.2. The calibration curve by using first-order absorption spectra for BY13 and RB in binary dye solutions.

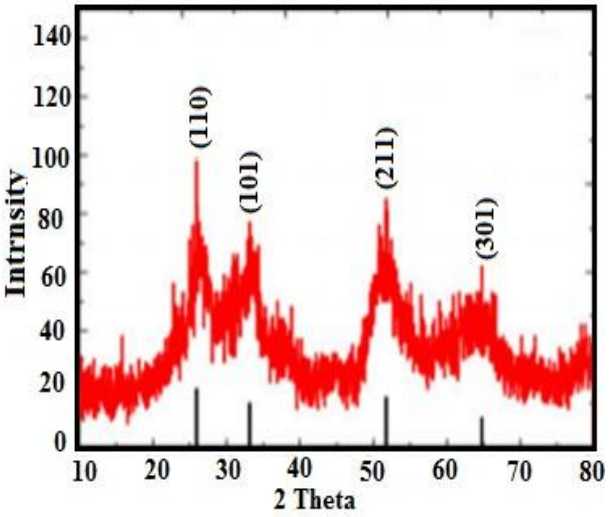

Fig.3. XRD pattern for SnO_2/AC

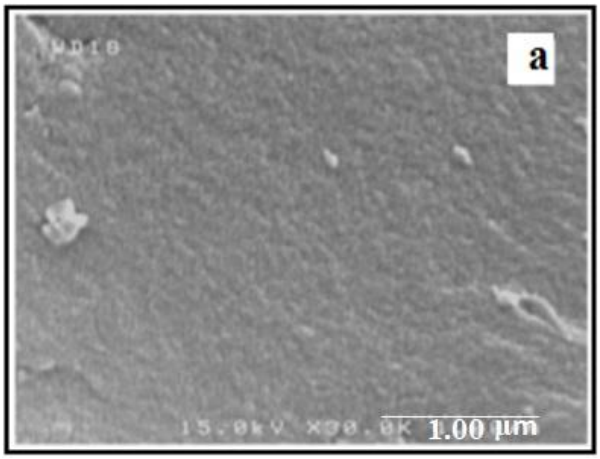

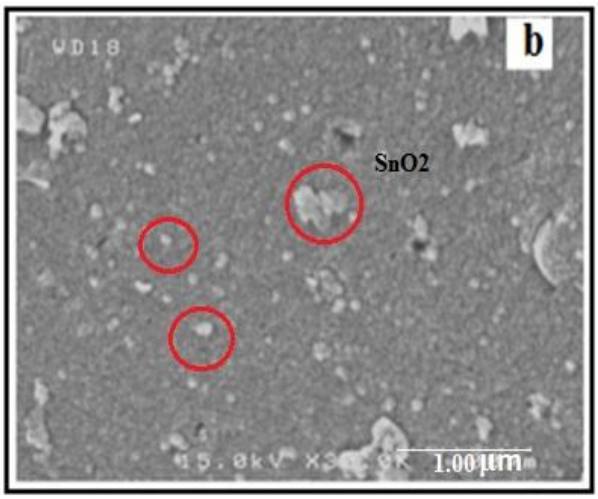

Fig.4. SEM images for (a) AC and (b)SnO_2/AC.

3.2. Photo-catalytic activity of SnO_2/AC

According to the band gap value of 3.75 eV for the SnO_2/AC nanocomposite [14], we can conclude that it is activated in the UV region. Fig.5 shows different UV

irradiation times for the photo-degradation of the dyes in the binary dye solution. According to this figure, the decrease in absorbance confirms the efficiency of the proposed dye photo-degradation process in the binary dye solution in the presence of the UV light and Sn_2O/AC catalyst.

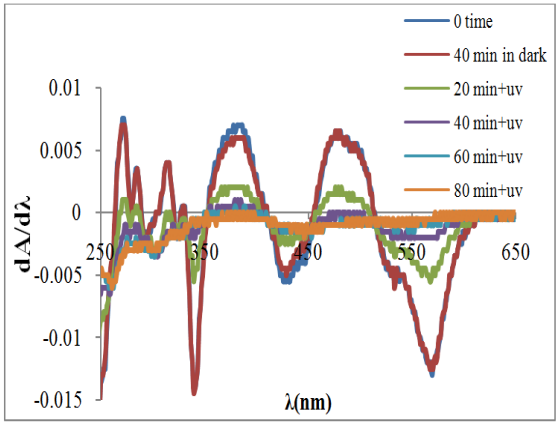

Fig.5. First-order absorption spectra for MO solution as a function of UV light exposition time. Conditions: 100 mL of binary solution, 12.0 mg L^{-1} of RB and 7 mg L^{-1} of BY13; catalyst dosage, 5 mg; and pH 5.5.

It is important to explain the effect of the catalyst in the photo-degradation process. The SnO_2 catalyst is a semi-conductor that acts as an electron and hole source. When the catalyst is exposed to light, the electrons and holes are created in the conduction and valence bands, respectively [17]. In this process, the electrons react with O_2 and the holes react with H_2O, which in turn produce the superoxide anion radicals and hydroxyl anion radicals. The radicals formed by hitting the dye molecules cause the molecules to break [18]. The best reason for using carbon as a support is the adsorption of dye molecules on the activated carbon sites, and eventually, their immediate photo-degradation. Therefore, the photo-catalytic activity increases [19].

3.3.Effect of pH on photo-degradation of binary dye solution

The effect of pH on the photo-degradation process is important. In this study, it was studied at the pH range of 4-8.5 for BY13 and RB. The NaOH and HCl solutions were used to adjust the pH of solution. The results shown in Figs.6 shows that the photo-degradation efficiency of the two dyes increases with the increment of pH up to 5.5, and then it decreases. Therefore, the optimum value for the solution pH was selected to be 5.5. As pH increased to 5.5, adsorption of the dyes on the anionic surface of the catalyst increased. Consequently, the degradation efficiencies increased [17]. At pH values higher than 5.5, the decrease in the photo-degradation may be due to the agglomerization of the catalyst [20].

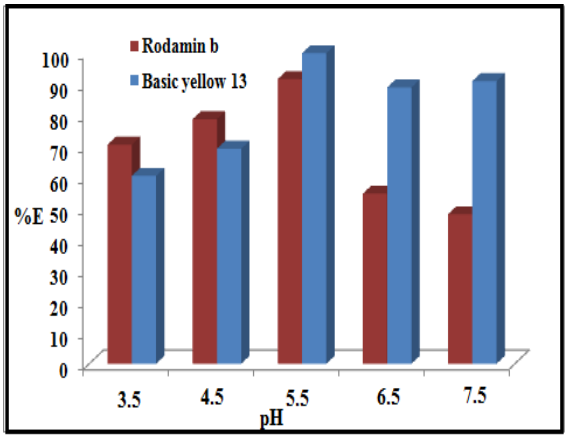

Fig.6. Effect of pH on photo-degradation of RB and BY13. Conditions: 100 mL mixture of two dyes with concentrations of 12 and 7 mgL^{-1} for RB and BY13, respectively; catalyst dosage, 5 mg; and irradiation time of 60 min.

3.4. Effect of initial concentration of dyes

In the current study, the effects of different concentrations of the two dyes on the photo-degradation efficiencies were investigated in the binary mixture of the basic yellow 13 (BY13) and rodamin b (RB) dyes with the concentration ranges of 3-15 and 7-15 mgL^{-1}, respectively. According to Fig.7, due to light absorption by dye molecules, with increase in the concentrations of the dyes, the photo-degradation efficiencies decreased [17].

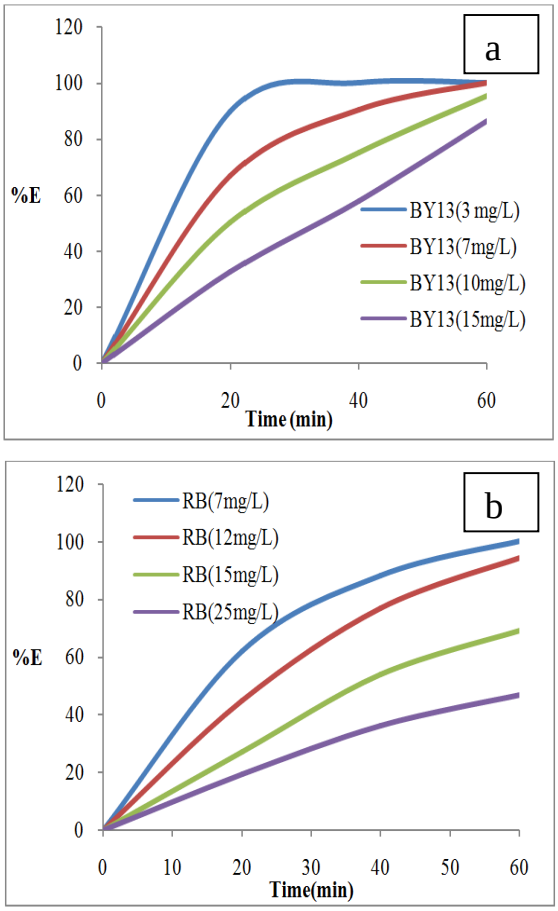

Fig.7. Effect of initial dye concentrations on degradation efficiencies of (a) BY13 and (b) RB.

Experimental conditions: catalyst dosage, 8 mg; V, 100 mL; pH 5.5.

3.5. Effect of dosage of SnO_2/AC catalyst

Effect of dosage of SnO_2/AC nanocomposite was investigated in the range of 2-12 mg with a pH value of 5.5, and certain dye concentrations (12 and 7 mgL^{-1} for RB and BY13, respectively). As shown in Fig.8, with increase in the catalyst dosage to 8 mg, the photo-degradation efficiencies increased, and then decreased. This phenomenon can be justified through two reasons: 1) the increment of catalyst dosage to 8 mg can improve the photo-degradation efficiency due to the increase in the active sites on the SnO_2/AC surface, 2) at higher than 8 mg of the catalyst, the photo-degradation efficiencies decreased due to dispersion of the UV light, which results in the reduction of the photons received by the catalyst [21, 22].

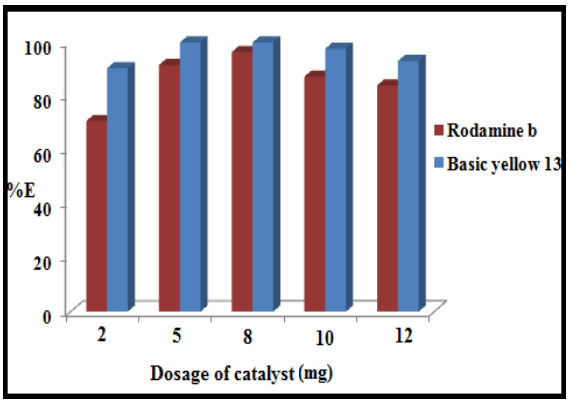

Fig.8. Effect of catalyst dosage on degradation efficiencies. Experimental conditions: 100 mL mixture of two dye with concentrations of 12 and 7 mgL^{-1} for RB and BY13, respectively, pH 5.5, irradiation time of 60 min.

3.6. Reuse of SnO_2/AC catalyst

In order to study the reusability of the catalyst, after separation from the dye solution, it was washed with distilled water and ethanol, and then used for the next experiments. The results shown in Table 2 revealed that the efficiency of the catalyst did not change appreciably after four times of use in the photo-degradation process.

Table 2. Results obtained for reuse of SnO_2/AC catalyst.

No. of used cycle	E%	
	BY13	RB
1	100	94.44
2	100	94.08
3	100	92.35
4	98.87	90.43
5	91.10	82
6	80.31	64

4. Conclusion

The SnO_2/AC nanocomposite as new photocatalyst was used successfully for the photo-degradation of the dyes RB and BY13 in their binary solution. In this work, AC, as a bed for SnO_2, plays an important role in the degradation process. When SnO_2 is placed on the surface of AC, the degradation efficiency is expected to increase because AC increases the surface area available for adsorbing the dye molecules. In addition to, under irradiation, the excited electrons in

AC are transferred to CB of SnO_2 and degradation efficiency increases. Also, in order to analyze the concentrations of the dyes in the binary solution, the derivative spectrophotometric method was used. Under the optimal experimental conditions, the greatest degradation efficiency was observed at pH 5.5, with a small amount of catalyst (8 mg) being used. Moreover, the catalyst had a reasonable performance after four reuses. The results obtained from this study confirmed a good performance of the catalyst in the photo-degradation of the dyes in their binary solution.

Acknowledgment

We wish to thank the department of chemistry in the Semnan University for supporting this work.

References

1. Kumar, P. S. S., Sivakumar, R., Anandan, S.; Madhavan, J., Maruthamuthu, P., Ashokkumar, M., , water research, 42 (2008) 4878-4884.

2. Tan, T. T. Y., Yip, C. K., Beydoun, D., Amal, R., Chem. Eng. J, 95 (2003) 179-186.

3. Bhattacharjee, A., Ahmaruzzaman, M., Sinha, T., Spectroc. Acta. A, 136 (2015**)** 751-760.

4. Cai, Z.-Q., Shen, Q.-H., Gao, J.-W., J. Inorg. Mater, 22 (2007) 733-736.

5. Zhu, L.-P., Bing, N.-C., Yang, D.-D., Yang, Y., Liao, G.-H., Wang, L.-J., Cryst. Eng. Comm, 13 (2011) 4486-4490.

6. Kim, S. P., Choi, M. Y., Choi, H. C., Applied .Surface .Science, 357 (2015) 302-308.

7. Namasivayam, C., Kavitha, D., Dyes. Pigments, 54 (2002) 47-58.

8. Aksu, Z., Tezer, S., Process. Biochem, 36 (2000) 431-439.

9. Xu, Y., Langford, C. H., Langmuir., 2001, 17 (3), 897-902.

10. Haque, S. A., Tachibana, Y., Willis, R. L., Moser, J. E., Grätzel, M., Klug, D. R., Durrant, J. R., J. Phys .Chem. B, 104 (2000) 538-547.

11. Stock, N. L., Peller, J., Vinodgopal, K., Kamat, P. V., Environ. Sci. Techno, 34 (2000) 1747-1750.

12. Ghaedi, M., Hajati, S., Barazesh, B., Karimi, F., Ghezelbash, G., J. Ind. Eng. Chem, 19 (2013) 227-233.

13. Turabik, M., J. Hazard. Mater., 2008, 158 (1), 52-64.

14. Davoodi, S., Marahel, F., Ghaedi, M., Roosta, M., Hekmati Jah, A., Desalin. Water. Treat, 52 (2014) 7282-7292.

15. Sajjadi, S. H., Goharshadi, E. K., J. Environ. Chem. Eng, 5 (2017) 1096-1106.

16. Taghavia, S., Asgharia, AR., Tavasoli, A., J.Appli. chemis, 41 (2017) 129-137.

17. A. Chamjangali, M., Bagherian, B., Bahramian, B., Fahimi Rad, B., Int. J. Environ. Sci. Technol, 12 (2015) 151-160.

18. Lin, H.-F., Liao, S.-C., Hung, S.-W., J. Photochem. Photobiol. A, 174 (2005) 82-87.

19. Andriantsiferana, C., Mohamed, E. F., Delmas, H., Environ. technol, 35 (2014) 355-363.

20. Gözmen, B., Turabik, M., Hesenov, A., J. Hazard. Mater, 164 (2009) 1487-1495.

21. Kaur, S., Singh, V., J. Hazard. Mater, 141 (2007) 230-236.

22. Sun, J., Wang, X., Sun, J., Sun, R., Sun, S., Qiao, L., J. Mol. Catal. A: Chem, 260 (2006) 241-246.